

FAULT IDENTIFICATION AND CLASSIFICATION OF POWER CABLES USING SHORT-TIME FOURIER TRANSFORMATION

Abhishek Pandey* and Nicolas Younan
 Department of Electrical and Computer Engineering
 Mississippi State University, Mississippi State, MS 39762, USA
 *Email: ap502@msstate.edu, younan@ece.msstate.edu

Abstract: Underground power cables encounter many different types of fault. Offline methods require power outages that are highly troublesome. The signal processing technique offers a viable diagnostic tool. In this paper, a diagnostic technique based on the short-time Fourier transform (STFT) for identifying and classifying different fault types is developed. In general, the STFT provides localization in both time and frequency that allows characterizing the frequency content of a time domain signal at each time instance. Note that the localization in time and frequency in this case is fixed. Three types of cables are used in this study: a normal cable, a shorted cable, and a cable with holes. The impedance in each case is computed via the STFT. In order to eliminate possible interference, various windowing is applied so that the resulting impedance magnitude and impedance phase can be examined in the frequency domain. A comparison with the Fourier transform results is also made to validate the applicability of this method. This comparative study reveals that the STFT is a better method for fault identification and classification than Fourier analysis.

1 INTRODUCTION

Manufacturing defects and/or environmental contact cause many different types of fault in the underground power cable. Predictive analytics are the next logical extension of the self-healing grid concept. Today, most equipment diagnostics are performed on de-energized equipments. In keeping with the Smart Grid vision, diagnostic techniques must be developed, which can be utilized so that decisions regarding replacement prior to failure can occur; thus minimizing impact to customers. Due to the impact of the aging infrastructure, and in particular underground polymeric cables, various offline and online methods have been developed for the detection of the remaining life of underground cables [1-2].

The offline methods require power outage, which can lead to further difficulty in their implementation. On the other hand, signal processing methods provide promising online techniques for the diagnostics of underground power cables. A common technique that is simple and easy to implement is the Fourier transform [3]. However, the Fourier transform provides information only about the frequency content (frequency spectrum) over the entire duration of the time domain signal. Thus, it is quite difficult to characterize the frequency content of the signal as time progresses.

In this paper, a diagnostic technique based on the short-time Fourier transform (STFT) for identifying and classifying different fault types is developed. In general, the STFT provides localization in both time and frequency that allows characterizing the frequency content of a time domain signal at each time instance. Note that the localization in time and frequency in this case is fixed.

2 METHODOLOGY

It is well known that the FFT, in general, is not a sufficient method for analyzing fault diagnostics. A more appropriate method to investigate is the short-time Fourier transform (STFT). The STFT [4] is a windowed version of the Fourier transform, i.e., its implementation is based on applying the Fourier transform to a sliding window of the time domain signal. Accordingly, the window choice is important to the quality of the localization. In general, the STFT is a complex function of time and frequency and its magnitude is displayed in the time-frequency plane, i.e., in a form known as the spectrogram. The frequency and time resolutions are inversely proportional to each other and there is a tradeoff between them. Thus, at any given point of time, one can select a large window size and concentrate on the frequency resolution, or one can select a small window size so that we can get a better time resolution. Mathematically, the STFT is represented by the following equation

$$\text{STFT}\{x(n)\} \equiv X(m,w) = \sum_{-\infty}^{\infty} x[n]w[n-m]e^{-jwn} \quad (1)$$

with w being a time domain window function. A common way of visualizing the STFT is the spectrogram, which is described by the square of the magnitude response of STFT. The spectrogram is represented mathematically as,

$$\text{spectrogram}\{x(t)\} \equiv |X(\tau,\omega)|^2 \quad (2)$$

The spectrogram is used in various signal processing applications, such as music and voice analysis. Some of the limitations of the spectrogram include the difficulty of extracting the

original signal since it contains no phase information.

2.1 Windowing

In implementing the STFT, five different types of windows [5], rectangular, Hamming, Hanning, triangular, and Gaussian, of length N (total number of samples) are used. A brief description of each window is presented below.

1. Rectangular window: This windowing has sharp edges at the extremes and not good in general because of the ripple effects that are introduced in the frequency response. This window is represented in the time domain by following equation.

$$w(n) = 1, n = 0, 1, \dots, N - 1, \quad (3)$$

2. Hamming window: This window has a smoother frequency and time domain responses. It is good because of its smooth frequency response output. The output equation is given by :

$$w(n) = 0.54 - \cos\left(\frac{2\pi n}{N-1}\right), n=0, 1, \dots, N-1 \quad (4)$$

3. Hanning window: Similar to the Hamming window, a Hanning window has smooth time domain and frequency domain responses. The Hanning window is represented mathematically by:

$$w(n) = 0.5 \left\{ \cos\left(\frac{2\pi n}{N-1}\right) \right\}, \quad (5)$$

$$n = 0, 1, \dots, N - 1$$

4. Triangular window: This windowing technique has a sharp edge response and has limited applications. It is represented by :

$$w(n) = 2/N \left\{ \frac{N}{2} - \text{abs}\left(n - \frac{N-1}{2}\right) \right\}, \quad (6)$$

$$n = 0, 1, \dots, N - 1$$

5. Gaussian window: The Gaussian window is another windowing technique that has smooth time domain and frequency domain responses. The Gaussian window is represented mathematically by:

$$w(n) = e^{-\frac{1}{2} \left\{ \left(\frac{n - \frac{N-1}{2}}{\alpha \frac{N-1}{2}} \right)^2 \right\}}, \quad (7)$$

$$n = 0, 1, \dots, N - 1$$

where $\alpha \leq 0.5$

2.2 Experimental data set

Five sets of data, with sample sizes of 5000 and 50000, are used in this study for three different cable types: normal cables, cables with a hole, and shorted cables. Data sets with 50000 samples are down-sampled to 5000 for uniformity. All the data is obtained from an $L=100$ m, $D=10.3$ mm AL, 4.45 mm XLPE cable (polymeric cable). Sampling of the data is done at time interval $t = 0.00000001$ sec.

3 RESULTS

From the 5 sample data sets that are available and for each type of the underground power cable (normal, shorted, and with holes), the 5th sample data set is used in this analysis for illustrative purposes. The STFT is used to obtain the magnitude and phase responses of the cable impedance.

The implementation of the STFT in this study is based on a window size of 128 samples, with 50% overlap (i.e., this corresponds to 64 overlapping samples). Note also that for the shorted cable, the time domain signal (voltage and current) consists of 50000 samples, whereas for the normal cables and cables with holes, 5000 samples are available. Thus, for comparison purposes, the shorted cable data are down-sampled (decimated) by a factor of 10 so that the data length for all three types of cables is the same. Considering the window size (128 samples) and the % overlap (64 samples) along with the available data length (5000 samples), the resulting STFT matrix size will be 65x77.

The results provided below correspond to the impedance magnitude and impedance phase for the three types of cables considered in this study for different types of windows. In this study, the results obtained from both methods (impedance computation via the sending end voltage and impedance computation via the differential voltage) are nearly identical. Accordingly, only the results of the impedance computed from the differential voltage are illustrated here. Figures 1-20 correspond to the magnitude response of the impedance as a function of time and frequency and the impedance phase as a function of frequency over a specified time window. With a 65x77 STFT matrix size, the phase response characteristic is selected as the phase response corresponding to the 32nd column of the STFT matrix. In all the phase response plots *blue* corresponds to the phase response of a normal cable, *red* corresponds to the phase response of a cable with hole, and *green* corresponds to the phase response of a shorted cable.

By examining these figures, it seems that the three different types of cables can be easily distinguished from the phase response for all windowing types with the Gaussian window having slightly better results in terms of both magnitude and phase responses.

The different types of cables are clearly distinguishable from the phase response. Additionally, the magnitude response for the shorted cable shows distinctive behavior in the spectrum. Similar behavior is also obtained for all datasets analyzed. This may be used for fault detection. However, further investigation is required.

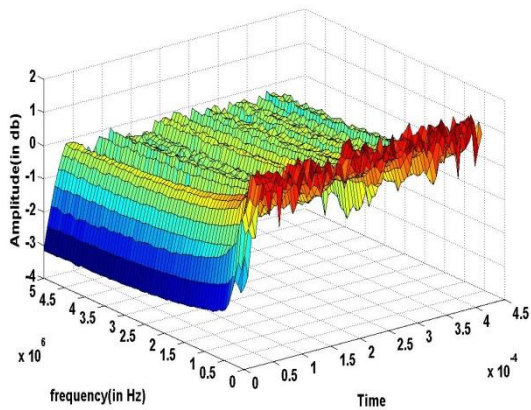


Fig 1: Impedance magnitude with a rectangular window (differential voltage, normal cable, dataset 5)

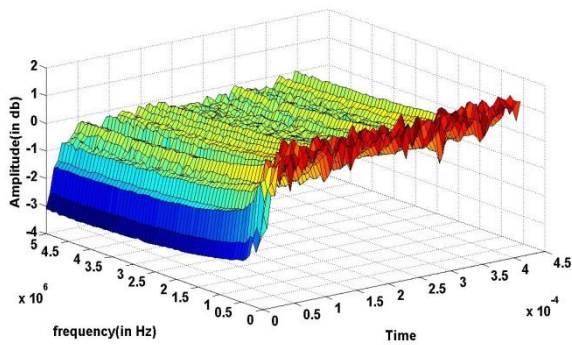


Fig 2: Impedance magnitude with a rectangular window (differential voltage, cable with holes, dataset 5).

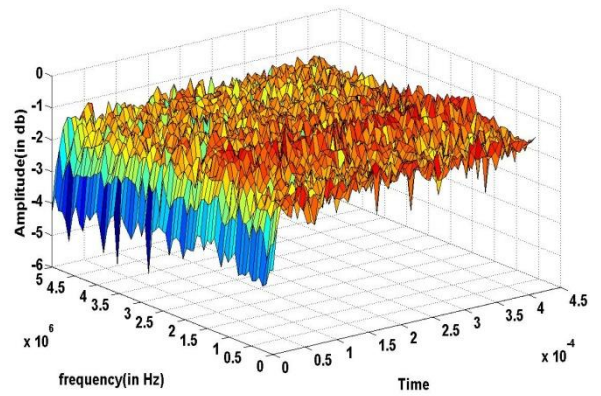


Fig 3: Impedance magnitude with a rectangular window (differential voltage, shorted cable, dataset 5)

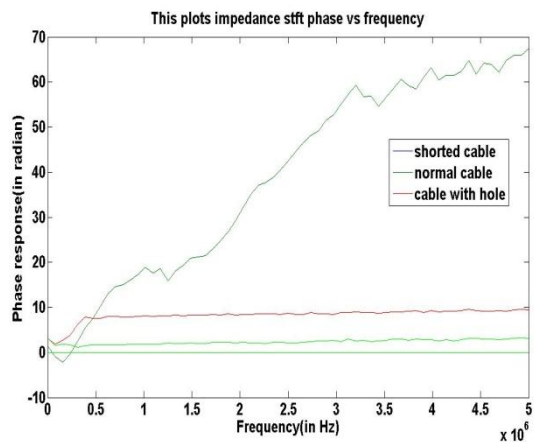


Fig 4: Impedance phase with a rectangular window (differential voltage, dataset 5)

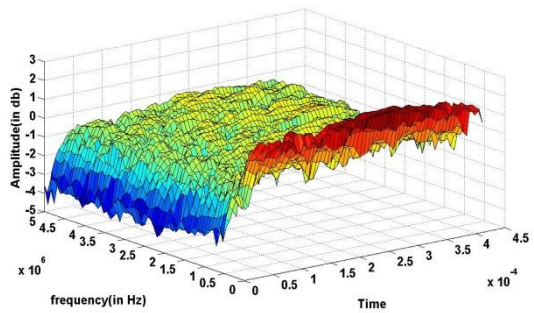


Fig 5: Impedance magnitude with a triangular window (differential voltage, normal cable, dataset 5)

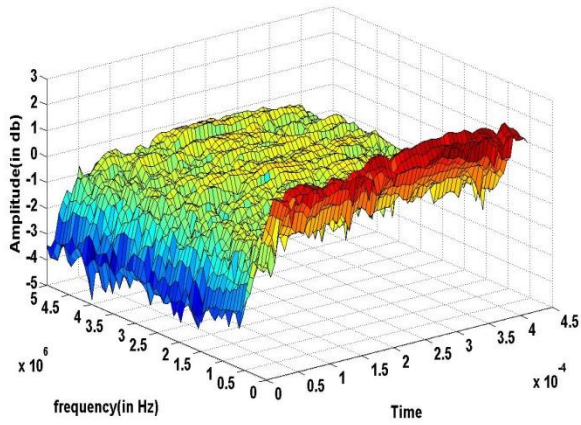


Fig 6: Impedance magnitude with a triangular window (differential voltage, cable with holes, dataset 5).

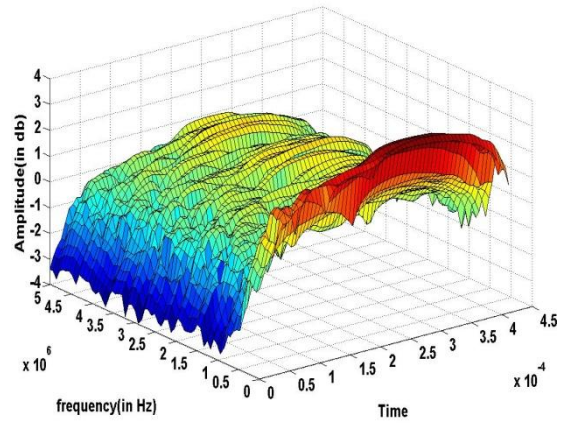


Fig 9: Impedance magnitude with a Hanning window (differential voltage, normal cable, dataset 5).

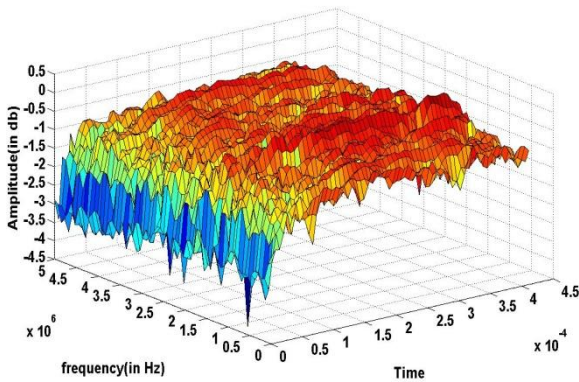


Fig 7: Impedance magnitude with a triangular window (differential voltage, shorted cable, dataset 5)

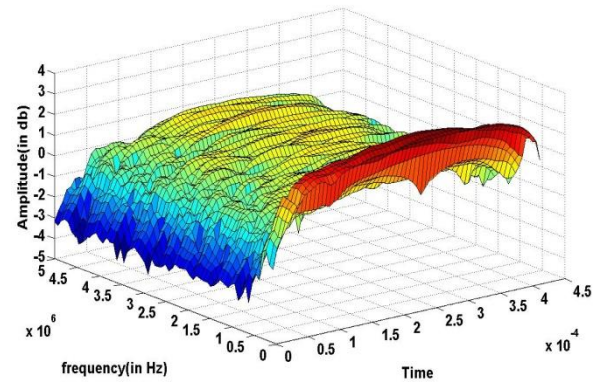


Fig 10: Impedance magnitude with a Hanning window (differential voltage, cable with holes, dataset 5).

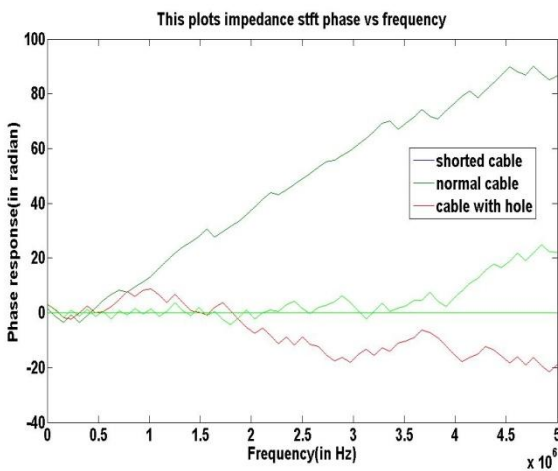


Fig 8: Impedance phase with a triangular window (differential voltage, dataset 5).

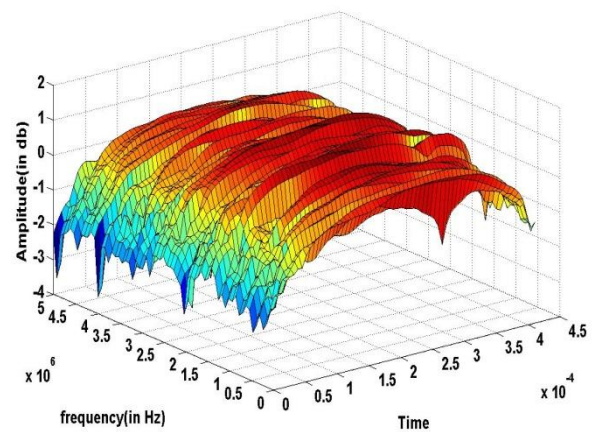


Fig 11: Impedance magnitude with a Hanning window (differential voltage, shorted cable, dataset 5).

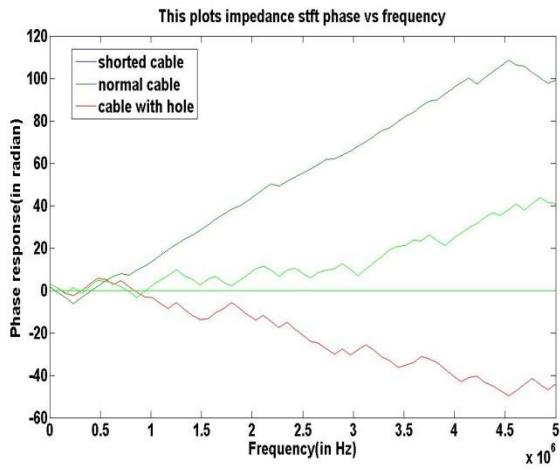


Fig 12: Impedance phase with a Hanning window (differential voltage, dataset 5).

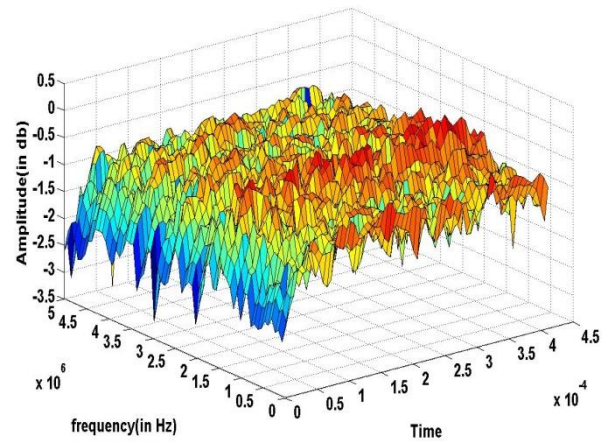


Fig 15: Impedance magnitude with a Hamming window (differential voltage, shorted cable, dataset 5).

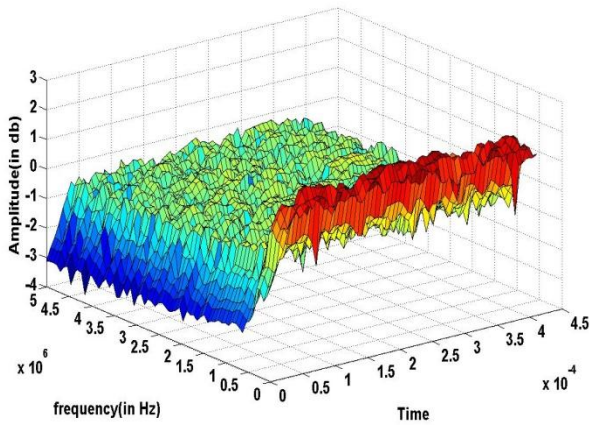


Fig 13: Impedance magnitude with a Hamming window (differential voltage, normal cable, dataset 5).

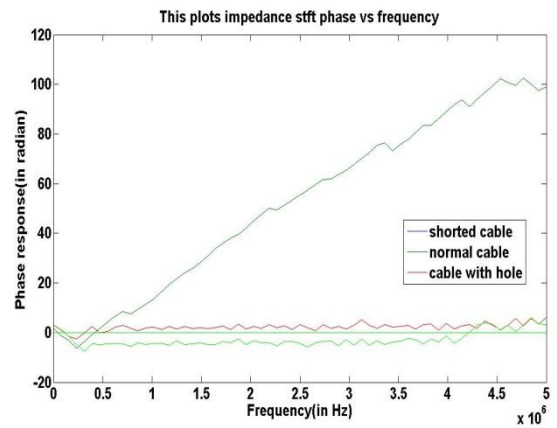


Fig 16: Impedance phase with a Hamming window (differential voltage, dataset 5).

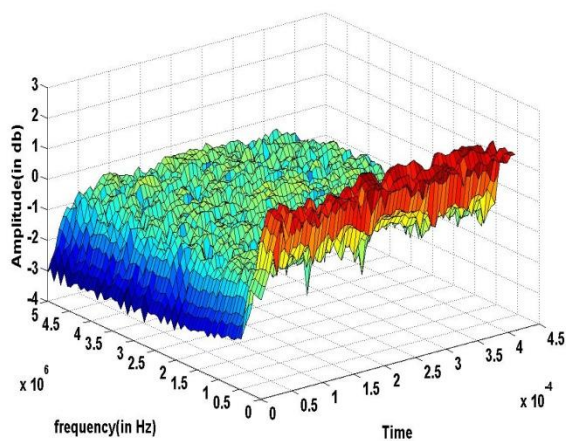


Fig 14: Impedance magnitude with a Hamming window (differential voltage, cable with holes, dataset 5).

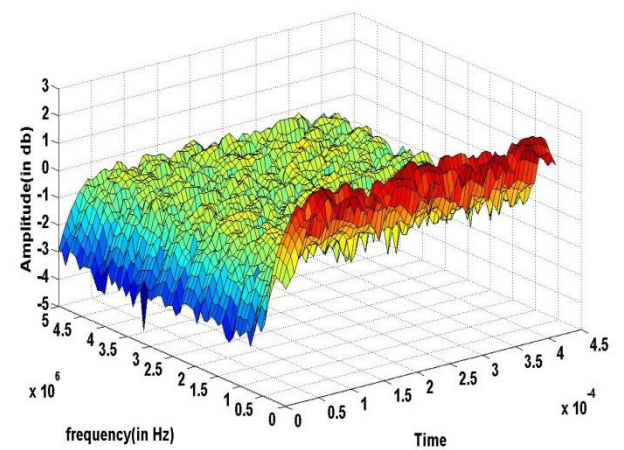


Fig 17: Impedance magnitude with a Gaussian window (differential voltage, normal cable, dataset 5).

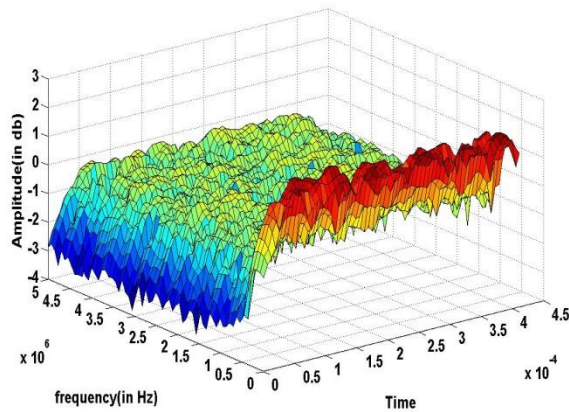


Fig 18: Impedance magnitude with a Gaussian window (differential voltage, cable with holes, dataset 5).

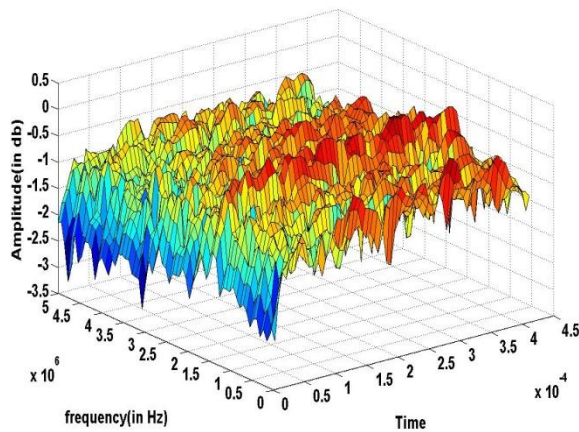


Fig 19: Impedance magnitude with a Gaussian window (differential voltage, shorted cable, dataset 5)

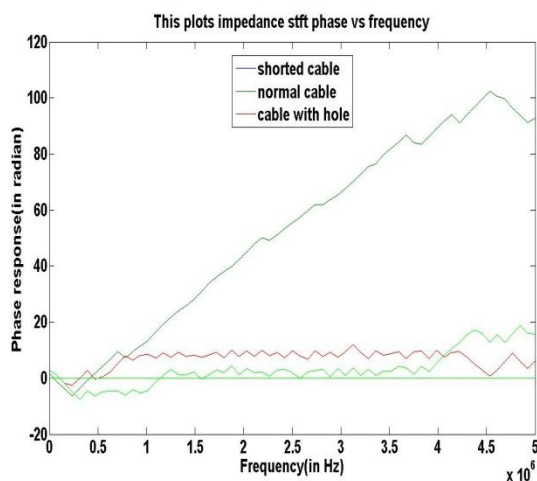


Fig 20: Impedance phase with a Gaussian window (differential voltage, dataset 5).

4 CONCLUSION

Both methods of impedance calculation (via the sending end voltage and the differential voltage) yield nearly identical results and can be used for differentiating between the different types of cable defects, especially from phase information. All windows types yield reasonable results. However, the Gaussian window seems to have slightly better results than the other windowing techniques in terms of noise reduction. However, both Hanning and Hamming windows are also good contenders for this type of applications as well. Accordingly, it is better to try out all three windows, Gaussian, Hanning, and Hamming, since the window choice is data dependent. The shorted cable can be easily distinguished directly from the magnitude response. The cable with holes and normal cable behave very similarly. However, they still can be distinguished from the magnitude response. Overall, the 3D visualization of the magnitude response enhances the distinction between the three different types of cables under investigation.

5 ACKNOWLEDGMENTS

The authors would like to acknowledge San Diego Gas & Electric (SDG&E) Company for sponsoring this research project. Special thanks go to Dr Thomas Bialek of SDG&E for his support.

6 REFERENCES

- [1] Thomas Owen Bialek, "Evaluation and modelling of high-voltage cable insulation using a high-voltage impulse," Ph.D. Dissertation, Mississippi State University, 2005.
- [2] C. K. Jung, J. B. Lee, X. H. Wang and Y. H. Song, "A study on fault location algorithm on underground power cable system," *Proceedings of IEEE Power engineering society general meeting*, pp 2165-2171, 2005.
- [3] Abhishek Pandey and Nicolas Younan "Underground Cable Fault Detection and Identification via Fourier Analysis," *International Conference on High Voltage Engineering and Application*, New Orleans, pp 618 – 621, 2010.
- [4] Francisco Jurado and José R. Saenz "Comparison between discrete STFT and wavelets for the analysis of power quality events," *Electric Power Systems Research* Volume 62, Issue 3, 28 July 2002, Pages 183-190.
- [5] Thomas Theußl, Helwig Hauser and Eduard Gröller "Mastering windowing: Improving Reconstruction," Institute of Computer Graphics, Vienna University of Technology.